applied sciences

MDPI

Article

Research on Road Characteristics and the Microscopic Mechanism of Lime–Phosphogypsum-Stabilized Red Clay

Ze-Yu Liu and Kai-Sheng Chen *

College of Civil Engineering, Guizhou University, Guiyang 550025, China; liuzeyu_1998@163.com
* Correspondence: chen_kaisheng@163.com

Abstract: In this paper, mixtures with different proportions of lime, phosphogypsum, and red clay were prepared, and the road properties and micromechanisms of lime–phosphogypsum-stabilized red clay were investigated by unconfined compressive strength test, water stability test, swelling test, shrinkage test, XRD quantitative analysis, and scanning electron microscope analysis. The results showed that the unconfined compressive strength of the mix increased and then decreased with the increase of phosphogypsum content. With the increase of age, the growth was faster in the first 14 days and basically stabilized in the last 14 days. The mixture has poor water stability, large absolute swelling rate, and low linear shrinkage. The reason for the increase of strength is that the reaction of lime, phosphogypsum, and red clay produces ettringite, and the cementing substance gels form a three-dimensional mesh skeleton structure; the excess of ettringite will cause the skeleton to expand and break, and the strength decreases.

Keywords: lime; phosphogypsum; red clay; road performance; microscopic mechanism

check for updates

Citation: Liu, Z.-Y.; Chen, K.-S. Research on Road Characteristics and the Microscopic Mechanism of Lime–Phosphogypsum-Stabilized Red Clay. *Appl. Sci.* **2023**, *13*, 8057. https://doi.org/10.3390/app13148057

Academic Editor: Eduardo Garzón

Received: 3 May 2023
Revised: 3 July 2023
Accepted: 6 July 2023
Published: 10 July 2023

Copyright: © 2023 by the authors. Licensee MDPI, Basel, Switzerland. This article is an open access article distributed under the terms and conditions of the Creative Commons Attribution (CC BY) license (https://creativecommons.org/licenses/by/4.0/).

1. Introduction

Phosphogypsum is a solid industrial waste produced during the production of phosphate fertilizer, and under normal circumstances, every 1 ton of phosphoramidite produced will generate about 5 tons of phosphogypsum. Guizhou, as one of the provinces with the largest production of phosphate fertilizer in China, generates about 5 million tons of phosphogypsum per year. At present, phosphogypsum treatment methods have mostly used land stacking and filling of rivers, lakes, and seas. These methods both encroach on the land and destroy vegetation, and leakage of acidic wastewater and some radioactive elements has caused pollution and endangered the health of human beings [1–4]. Red clay is a special clay that exhibits many fissures, high shrinkage, and high water sensitivity, and these features affect the application of red clay in highway engineering [5–9]. Most of the current studies on phosphogypsum treatment problems have applied phosphogypsum in construction and road foundation projects [10–15]. By mixing phosphogypsum with other substances to modify the treatment of different soil types, the soil properties can be enhanced and used for road base filling [16–18]. Applying phosphogypsum and red clay to subgrade pavement solves the problem of phosphogypsum pollution and improves the poor engineering characteristics of red clay, which has important scientific significance and applied engineering value. Many scholars have conducted some research on the application of phosphorus-containing solid waste on roads. Rakesh Kumar Duttaa et al. [19] proved that the lime–fly ash mixture with phosphogypsum cured for 28 days can be used as the base course and sub-base course of roads through unconfined compressive strength tests and indirect tensile strength tests. Kumar et al. [20] prepared lime–fly ash–phosphogypsum mixtures with different ages after three different curing treatments and applied unconfined compressive strength tests and unconsolidated undrained triaxial tests. According to the results of unconfined compressive strength, deviatoric stress, cohesion, friction angle, initial tangential modulus, and secant modulus obtained from the test, the lime–fly ash–phosphogypsum mixture can be applied to the subgrade. Kargar

et al. [21] mixed different proportions of gypsum in clay and conducted laboratory tests. They believed that the maximum dry bulk density decreased, the optimal water content increased, and the strength and CBR values increased significantly with increasing gypsum content. Tang et al. [22] conducted indoor and field tests on the feasibility and mechanical properties of phosphogypsum used in roadbed and pavement engineering. After many indoor tests, they found that phosphogypsum exhibited the minimal expansion, good water stability, and high strength necessary for use in roads. Xu et al. [23–25] discussed the drying and shrinkage characteristics of phosphogypsum, fly ash, lime, and clay mixtures used as base materials. From the perspective of drying and shrinkage characteristics, this mixture was combined with gypsum and deemed feasible for use as a pavement base material; the best mixing ratios for phosphogypsum–fly ash–lime–clay mixtures (phosphogypsum: fly ash: lime: clay) were 15:20:6:59 and 15:25:8:52. The above research showed that phosphogypsum has good prospects for applications in highway engineering. At present, there are few studies on the road performance and micromechanisms of phosphogypsum-stabilized red clay. In this paper, lime, phosphogypsum, or phosphogypsum and red clay is used to prepare mixtures in different proportions, the strength characteristics, water stability, swelling and shrinkage of phosphogypsum-stabilized red clay are probed through XRD quantitative analysis and scanning electron microscope (SEM), which revealed the mechanism for changes in the microstructure and provided technical support for applications of lime–phosphogypsum-stabilized red clay in highway engineering.

2. Materials and Methods

2.1. Raw Material Properties

2.1.1. Red Clay

The red clay used in this study was taken from the reconstruction and expansion project of Niuchang–Daoping Highway in Fuquan City, China. The soil sampling depth was approximately 3 m. The color of the soil sample was yellow-brown, the soil quality was uniform, the soil sample was moist, the structure was relatively dense, and there was a small amount of vegetation. Rhizomes and gravel were present. The basic physical indicators are shown in Table 1, the chemical composition is shown in Table 2, and the particle size distribution curve is shown in Figure 1.

Table 1. Basic physical and mechanical indexes of red clay.

Natural Moisture Content/(%)	Natural Wet Density/(g/cm^3)	Natural Dry Density/(g/cm^3)	Nonuniformity Coefficient	Curvature Coefficient	Specific Gravity
46.89	1.64	1.10	1.1	2.86	2.61
Plastic limit/(%)	Liquid limit/(%)	Plasticity Index	Optimal moisture content/(%)	Maximum dry density/(g/cm^3)	
44.82	77.03	32.21	30.41	1.452	

Table 2. Chemical composition of red clay.

Chemical Composition	SiO_2	Al_2O_3	Fe_2O_3	K_2O	MgO	TiO_2	CaO
Mass fraction (%)	54.159	28.697	10.358	3.085	1.493	1.302	0.300
SO_3	P_2O_5	MnO	Na_2O	V_2O_5	Cr_2O_3	PbO	other
0.170	0.116	0.096	0.076	0.054	0.020	0.015	0.06

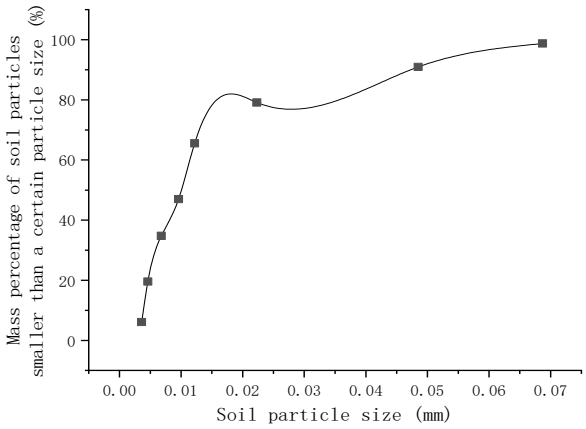


Figure 1. Particle size distribution curve of red clay.

2.1.2. Phosphogypsum

Phosphogypsum was taken from the Wengfu Phosphate Mine Storage Yard in Fuquan City, China. It was off-white and mostly in powder form, as shown in Figure 2. The basic physical indicators are shown in Table 3, and the chemical composition is shown in Table 4.



Figure 2. Phosphogypsum.

Table 3. Physical and mechanical properties of phosphogypsum.

Detection Indicator	Fineness /(%)	Density /(g/cm^3)	Specific Surface Area/(m^2/kg)	Water Content/(%)	Ignition Loss/(%)	Alkali Content/(%)	SO_3 Quality Score/(%)
Test results	44.3	2.38	102	5.3	18.43	1.31	0.07

Table 4. Chemical composition of phosphogypsum.

Chemical Composition	SO_3	CaO	SiO_2	F	P_2O_5	Na_2O	Al_2O_3
Mass fraction (%)	49.07	40.07	5.78	1.89	1.35	0.587	0.435
Fe_2O_3	MgO	Cl	SrO	K_2O	BaO	TiO_2	other
0.210	0.195	0.0955	0.0901	0.0744	0.0711	0.0420	0.0399

2.1.3. Lime

Lime was purchased from a manufacturer in Fuquan; it was a dry, white powder without agglomeration, and the main component was CaO. See Table 5 for details.

Table 5. Chemical composition of lime.

Substance	CaO	SiO_2	Na_2O	MgO	SO_3	Al_2O_3	Fe_2O_3
Mass fraction (%)	97.95	0.460	0.439	0.384	0.382	0.122	0.0831
SrO	Cl	CeO_2	Ag_2O	P_2O_5	TiO_2	Dy_2O_3	other
0.0325	0.0279	0.0222	0.0172	0.0145	0.0139	0.0106	0.0411

2.2. Mixture Ratio Design

According to the "Technical Guidelines for Construction of Highway Roadbases" (JTG/T F20-2015) [26], the lime dosage of lime-stabilized materials is not less than 10%. In addition, many scholars have performed research on the effects of mixing lime as an additive with phosphogypsum. Hu Wenhua [27] used lime to improve the red clay content of the Jiangxi Expressway, and the improvement was optimal when the lime content was 5–10%. Zhang Yingfu [28] conducted research on gypsum fly ash and lime binder and found that when the lime content was 6–8%, the strength was the best, and the material could be used as a pavement subbase material. Yang Heping [29] used quicklime to improve high liquid limit soil, and the results showed that when the lime content was 4–6%, the high liquid limit soil exhibited good road performance and met the requirements for highway subgrade filling. Therefore, the lime content was initially set at 6%, 8%, and 10%.

Based on research [30,31] designed to set two series of ratios, the first one was set with lime to phosphogypsum ratios of 1:1, 1:2, and 1:3. In order to use more phosphogypsum, the second series was set with phosphogypsum to soil mass ratios of 1:1, 1:2, and 1:3. The results are shown in Table 6. The proportions in the mixing ratios represent the percentage of each substance in the total mass of the mixture. According to the method designed for the mixture ratios in Table 6, unconfined compressive strength tests, expansion tests, and shrinkage tests were carried out indoors to analyze the mechanical properties of lime–phosphogypsum-stabilized red clay. On this basis, XRD and SEM were used to further explore the microstructure of the mixture.

Table 6. Mixture ratio design.

L/%	P/%	T/%	K/%	ω/%
6	6	88	90, 92, 93, 94, 95	27.11
	12	82		28.85
	18	76		28.42
	24	70		27.55
	31	63		28.52
	47	47		23.98
8	8	84		30.24
	16	76		28.01
	24	68		27.41
	23	69		27.84
	31	61		27.59
	46	46		25.94
10	10	80		28.16
	20	70		29.46
	30	60		28.55
	23	67		29.12
	30	60		28.55
	45	45		22.11

L = Lime, P = Phosphogypsum, T = Red clay, K = Compaction degree, and ω = Optimal moisture content.

2.3. Experiment Method

2.3.1. Unconfined Compressive Strength Tests

After passing the red clay and phosphogypsum through a 2 mm sieve, the red clay, lime, and phosphogypsum were weighed according to the ratios in Table 5 and mixed evenly. Then, a certain amount of water was added according to the corresponding moisture content, and the mixture was mixed. The raw materials were sealed and placed to make the moisture distribution even, and the samples preparation was started after standing overnight. Samples preparation was completed within 1 h using the static compaction method. The samples were cylinders with a height of 80 mm and a diameter of 39.1 mm [32]. After a sample was prepared, it was placed in a curing box with a temperature of 20 ± 2 °C and a relative humidity of 95% or more for 7, 14, and 28 days, and then unconfined compressive strength tests were carried out.

2.3.2. Water Stability Test

Sample preparation was the same as that used for the unconfined compressive strength tests. The samples were placed in a curing room with the temperature of 20 ± 2 °C and relative humidity of 95% or above for 6 days, and then they were immersed in water for 1 day to observe the degree of damage and carry out the unconfined compressive strength test on the complete sample [33].

2.3.3. Expansion Test

The static compaction method was used to prepare ring knife samples with the ratios in Table 6, the ring knife sample and dilatometer are shown in Figure 3. The sample was put into the dilatometer to start the test, water was poured into the dilatometer and entered the sample from bottom to top, and the water surface level was kept 5 mm higher than the test sample. The start time was recorded when water was injected, and compression was applied for 5 min, 10 min, 20 min, 30 min, 1 h, 2 h, 3 h, or 24 h, and then indicator readings were taken for 24 h or until sample expansion was not more than 0.01 mm within a 2 h interval. Then, deformation was deemed stable, and the test was terminated [33].



(**a**) (**b**)

Figure 3. Ring knife sample and dilatometer for expansion test. (**a**) Ring knife sample; (**b**) Dilatometer.

The absolute expansion was calculated according to Formula (1):

$$\delta_t = \frac{h_t - h_0}{h}, \quad (1)$$

where δ_t is the Absolute expansion rate at time t (%);
h_0 is the scale reading at the beginning of the test (mm);
h_t is the scale reading at time t (mm); and
h is the initial height of the sample (mm).

2.3.4. Shrink Test

The static compaction method was used to prepare ring knife specimens with the proportions shown in Table 6. The sample was put into the shrinkage tester at a temperature of 25 °C and compressed for 1 h, 2 h, 3 h, 4 h, or 24 h. After that, the dial indicator was read every 24 h. When the dial indicator reading remained unchanged for 2 h, sample contraction was considered to be stable. The linear shrinkage rate is the ratio of the vertical shrinkage deformation of the soil to the height of the original soil sample. To determine the linear shrinkage rate of the mixture, a sample preparation test was carried out in accordance with the "Test Methods of Soils for Highway Engineering" (JTG 3430-2020) [33].

The line shrinkage rate was calculated as follows:

$$\delta_t = \frac{H_t - H_0}{H} \times 100, \quad (2)$$

where δ_t is the shrinkage rate of the sample line at a certain moment in the shrinking process (%);

H_t is the dial indicator reading at a certain time during contraction (mm);

H_0 is the initial reading of the dial indicator (mm); and

H is the initial height of the sample (mm).

2.3.5. Microstructure Test

Before sample preparation, the mass of the sample was calculated according to the volume of the ring cutter and the corresponding ratio in Table 6. The mixing ratio was the same as that used in the unconfined test, and then the mixture of predetermined quality was weighed, poured into the sample preparation device, and subjected to static pressure molding. The diameter of the sample was 61.8 mm and the height was 20 mm, which is the same as that of the expansion test sample. After the sample was prepared, it was placed in a constant temperature and humidity curing box with a temperature of 20 ± 2 °C and a humidity of 95% for curing. After 7 days, the sample was removed from the ring knife. XRD component quantitative analyses were performed with the central core part of the sample.

SEM samples were broken into pieces measuring approximately 2 cm^3, and knife cutting was not allowed. The soil block was sanded with coarse sandpaper first and then with fine sandpaper so that the soil block was ground into soil slices of approximately 0.5 cm^3. The thinner the soil slice was, the clearer the image. During polishing, tiny powder particles were generated on the soil surface. Scotch tape was used to remove the powder on the surface until the surface of the sample was clean. Because the conductivity of phosphogypsum-stabilized red clay is poor, gold spraying was required before scanning. Only in this way could the images be observed well.

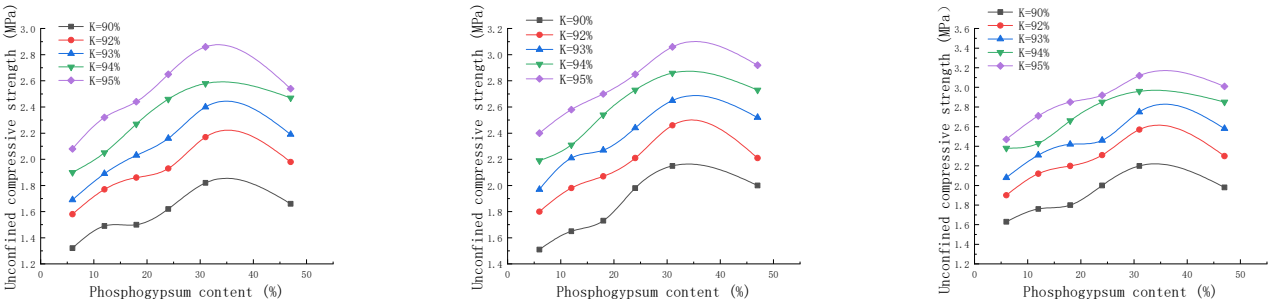
3. Results

3.1. Analysis of Unconfined Compressive Strength Results

3.1.1. Influence of the Phosphogypsum Content on Unconfined Compressive Strength

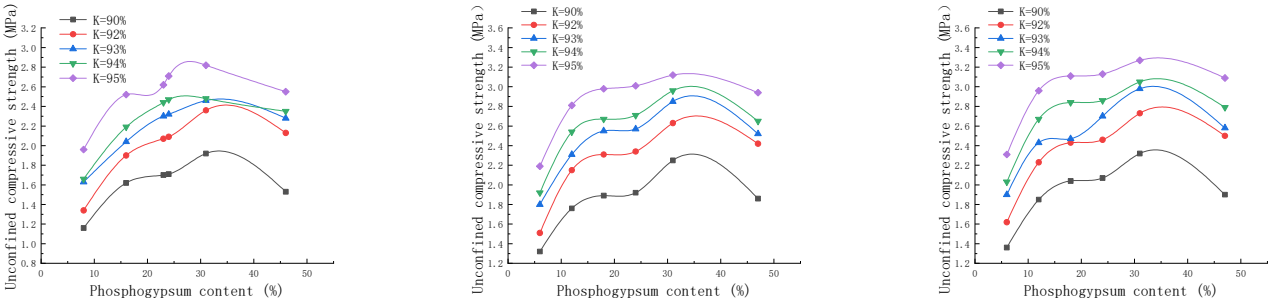
Figures 4–6 and Table 7 show that the unconfined compressive strength of the 7 d, 14 d, and 28 d phosphogypsum-stabilized red clay samples at each compaction degree increased first and then decreased with increasing phosphogypsum content. When the lime content was 6%, the unconfined compressive strength was largest when the phosphogypsum content was 31%. At this point, the ratio lime:phosphogypsum = 1:5.2; when the lime content was 8%, the maximum unconfined compressive strength occurred when the phosphogypsum content was 31%. The maximum strength was obtained when the ratio lime:phosphogypsum = 1:3.9; when the lime content was 10%, the unconfined compressive strength was largest when the content of phosphogypsum was 23% and when lime:phosphogypsum = 1:2.3. At the same age and with the same degree of compaction, the addition of more lime provided greater unconfined compressive strength for the mixture. Lime reacts in the mixture to produce hydrated calcium silicate and hydrated calcium alu-

minate, which improves the strength of the mixture while the reaction of phosphogypsum will produce ettringite to further improve the strength of the mixture. With the increase of phosphogypsum to produce too much ettringite, it will lead to the destruction of the mix structure, thus reducing the strength.



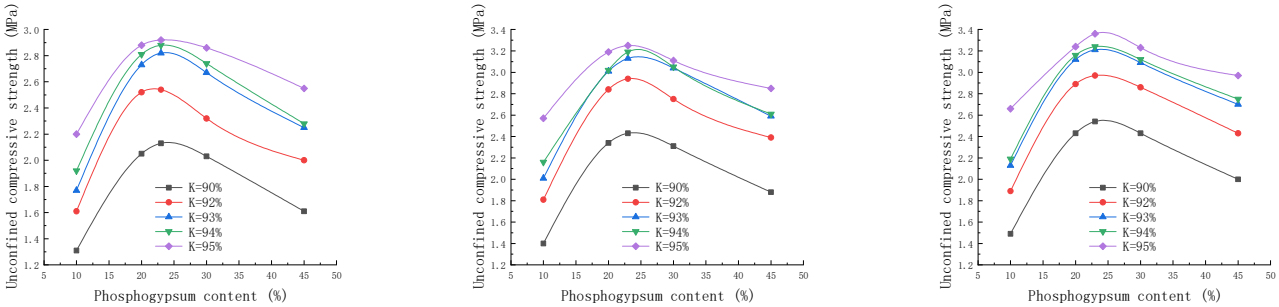
(**a**) (**b**) (**c**)

Figure 4. Relationship between phosphogypsum content and unconfined compressive strength with lime content L = 6%. (**a**) 7 d unconfined compressive strength; (**b**) 14 d unconfined compressive strength; (**c**) 28 d unconfined compressive strength.



(**a**) (**b**) (**c**)

Figure 5. Relationship between phosphogypsum content and unconfined compressive strength with lime content L = 8%. (**a**) 7 d unconfined compressive strength; (**b**) 14 d unconfined compressive strength; (**c**) 28 d unconfined compressive strength.



(**a**) (**b**) (**c**)

Figure 6. Relationship between phosphogypsum content and unconfined compressive strength with lime content L = 10%. (**a**) 7 d unconfined compressive strength; (**b**) 14 d unconfined compressive strength; (**c**) 28 d unconfined compressive strength.

Table 7. Maximum unconfined compressive strengths (K = 90%).

L (%)	P (%)	7 d Unconfined Compressive Strength (MPa)	14 d Unconfined Compressive Strength (MPa)	28 d Unconfined Compressive Strength (MPa)
6	31	1.82	2.15	2.20
8	31	1.92	2.25	2.32
10	23	2.03	2.31	2.43

3.1.2. Influence of Age on Unconfined Compressive Strength

Due to space limitations, this article only shows the relationship between unconfined strength and the age of the mixture for the 8% lime group, and the admixture change law for the other groups was basically the same.

Figure 7 shows that with increasing age, the unconfined compressive strength of the mixture increased; the increase was faster during the first 14 days and slower during the latter 14 days. Taking a sample with 8% lime + 31% phosphogypsum and 90% compaction as an example, the unconfined compressive strength after 7 d was 1.92 MPa, the unconfined compressive strength after 14 d was 2.25 MPa, and the unconfined compressive strength after 28 d was 2.41 MPa; the 7 d unconfined compressive strength reached 79.67% of the 28 d unconfined compressive strength, and the 14 d unconfined compressive strength reached 93.36% of the 28 d unconfined compressive strength. The increase in the maintenance time of the mixture leads to a more adequate hydration reaction of the lime in the mixture, which results in an increase in the unconfined compressive strength.

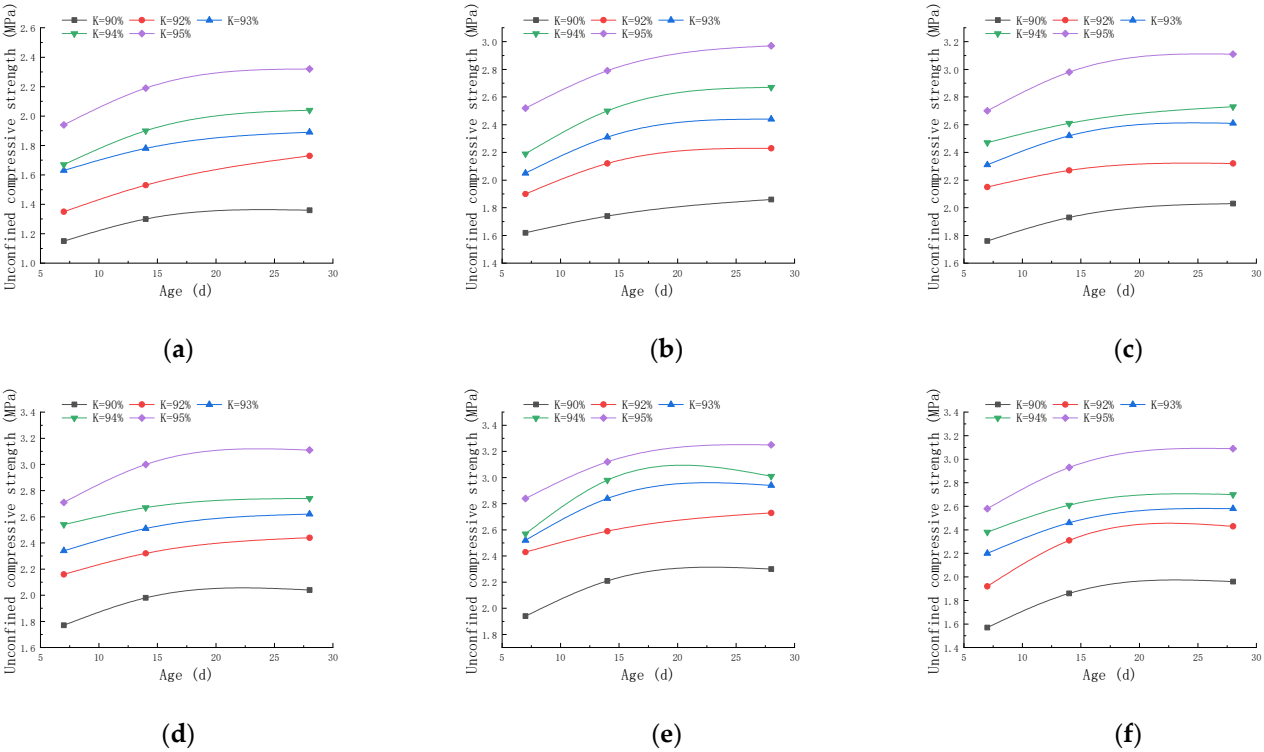


Figure 7. Relationship curves for unconfined compressive strength and age of the mixture (L = 8%). (**a**) P = 8%; (**b**) P = 16%; (**c**) P = 23%; (**d**) P = 24%; (**e**) P = 31%; (**f**) P = 46%.

3.2. Analysis of Water Stability Test Results

Due to space limitations, this article only shows experimental water stability results for mixtures in the 8% lime content group.

Figures 8 and 9 show that the water stabilities of the mixtures were very poor. Soil particles gradually fell off after the sample was soaked in water for only approximately 10 s.

After the sample with P = 24% was soaked in water for 120 s, 15% of the sample volume fell off, and after the sample with P = 31% was soaked in water for 120 s, the lost volume was 12%. After 24 h of soaking in water, all soil particles fell off and were seen at the bottom of the container; the samples did not exhibit strength. However, from the perspective of the shedding speed of soil particles, the higher the phosphogypsum content was, the better the water stability of the mixture.



(**a**) (**b**) (**c**)

Figure 8. 8%L + 24%P + 68%T, K = 90%. (**a**) Soaked in water for 10 s; (**b**) Soaked in water for 120 s; (**c**) Soaked in water for 24 h.



(**a**) (**b**) (**c**)

Figure 9. 8%L + 31%P + 61%T, K = 90%. (**a**) Soaked in water for 10 s; (**b**) Soaked in water for 120 s; (**c**) Soaked in water for 24 h.

3.3. Analysis of Expansion Test Results

Due to space limitations, the relationship of absolute expansion rate of the mixture with time was analyzed for samples with 8% lime content, and the results are shown in Figure 10. The changes in the contents of other groups were basically the same.

Figure 10 shows that when the lime content was 8%, the absolute expansion rate of the mixture increased with time, and the expansion had not yet reached stability at 223 h. At this time, the absolute expansion rates of the mixtures with different phosphogypsum contents ranged from 38% to 55%.

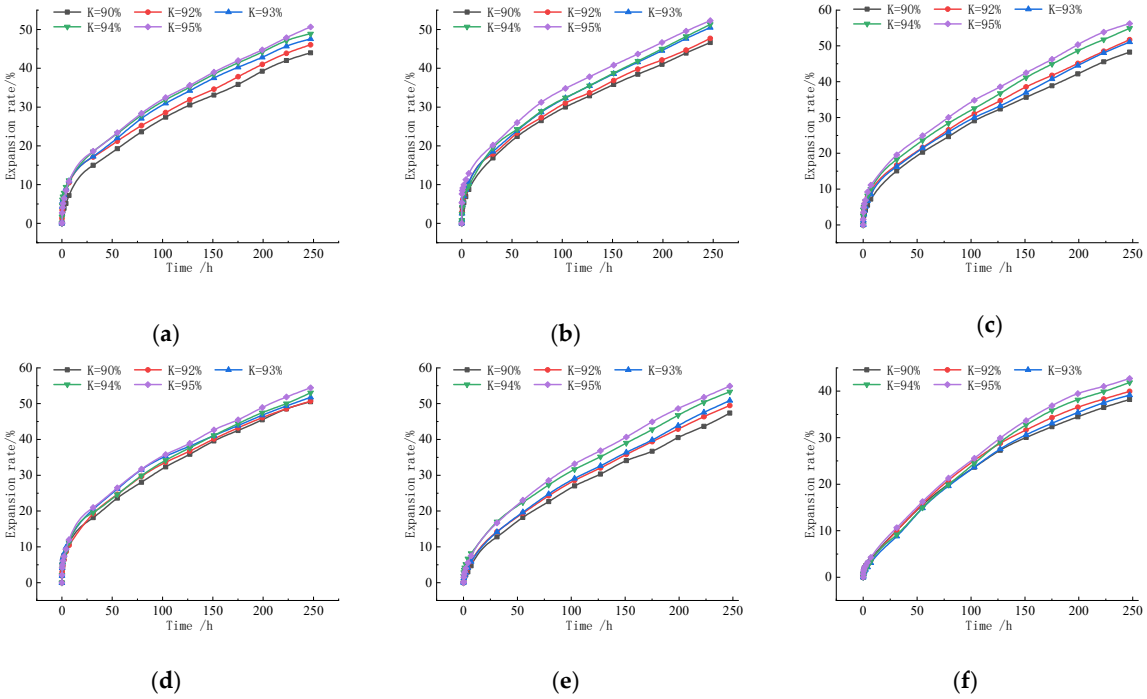


Figure 10. Relationship curves for absolute expansion rates of lime–phosphogypsum-stabilized soils and time (L = 8%). (**a**) 8%L + 8%P + 84%T; (**b**) 8%L + 16%P + 76%T; (**c**) 8%L + 23%P + 69%T; (**d**) 8%L + 24%P + 68%T; (**e**) 8%L + 31%P + 61%T; (**f**) 8%L + 46%P + 46%T.

It can be clearly seen from Figure 11 that with the increase of phosphogypsum content, the absolute expansion rate of lime–phosphogypsum-stabilized red clay presents a trend of first increasing and then decreasing, and the greater the compaction degree is when the content of phosphogypsum is the same, the greater the absolute expansion rate of the mixture. For example, when the lime content is 8%, when K = 90%, the absolute expansion rate of lime:phosphogypsum = 1:2.8 reaches the maximum; when K = 95%, the absolute expansion ratio of lime:phosphogypsum = 1:3.0, the absolute expansion rate reaches a maximum. The samples with different degrees of compaction reach their maximum value between lime:phosphogypsum = 1:2.8 and 1:3. Phosphogypsum–lime-stabilized red clay's absolute expansion rate is affected by the cementitious material and ettringite content, with the phosphogypsum content increases to generate ettringite, which destroys the mix structure, causing the mix to produce greater expansion; phosphogypsum content is too much, the mix PH value decreases, generating less ettringite, while the mix has a low content of viscous particles, the mix expansion is reduced.

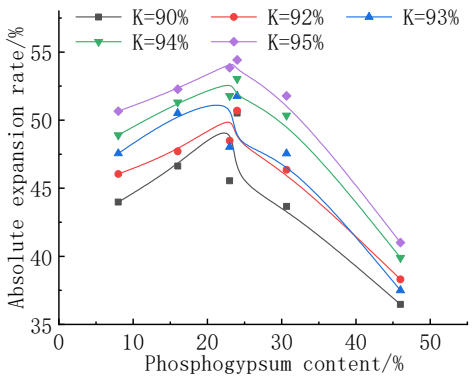


Figure 11. Relationship between absolute expansion rate of the mixture and phosphogypsum content (L = 8%).

3.4. Analysis of Shrink Test Results

Due to space limitations, the linear shrinkage rate of the mixture as a function of time was analyzed for a lime content of 8%, and the changes in the other groups were basically the same.

Figure 12 shows that the line for shrinkage rate first increased rapidly, then increased slowly with time and finally stabilized, and the final shrinkage rate was between 0.8% and 2.2%. For example, in (c) shrinkage of the K = 90% sample increased rapidly from 0 to 1.9% in the first 10 h and then increased slowly before reaching approximately 2.4% at 35 h, and subsequent shrinkage tended to be flat with time.

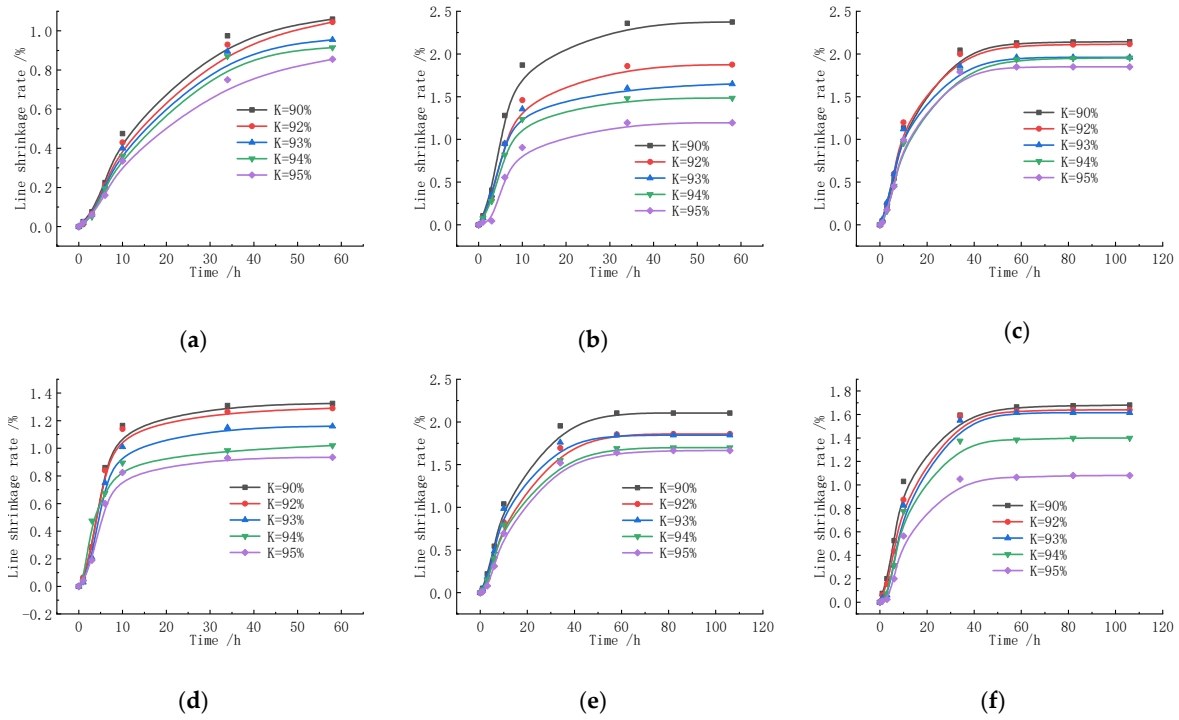


Figure 12. Relationship between the linear shrinkage of the mixture and time (L = 8%). (**a**) 8%L + 8%P + 84%T; (**b**) 8%L + 16%P + 76%T; (**c**) 8%L + 23%P + 69%T; (**d**) 8%L + 24%P + 68%T; (**e**) 8%L + 31%P + 61%T; (**f**) 8%L + 46%P + 46%T.

Figure 13 shows that the linear shrinkage rate of the mixture first increased and then decreased with increasing phosphogypsum content. For example, when the phosphogypsum content is 19.44%, the sample line shrinkage of 90% compaction reaches the maximum value of 2.22%; when the content of phosphogypsum increases to 23.62%, the sample line shrinkage of 92% compaction reaches the maximum value of 2.03%; when the phosphogypsum content is 26.14%, the linear shrinkage rate of the 95% compaction sample reaches the maximum value of 1.74%, and the mixture of different compaction degrees reaches the maximum value between lime:phosphogypsum = 1:2–1:3, and then decreasing gradually. When the content of phosphogypsum is low, lime will neutralize the acidity in the mixture, so that the formation of gelatinous substances and the content of ettringite will be reduced, and the change of viscous particles in the mixture is small, so the line shrinkage rate of the mixture increases. When the phosphogypsum content is high, as the phosphogypsum continues to increase, the gelling material, ettringite, and clay particles in the mixture continue to decrease, resulting in a decrease in the linear shrinkage of the mixture.

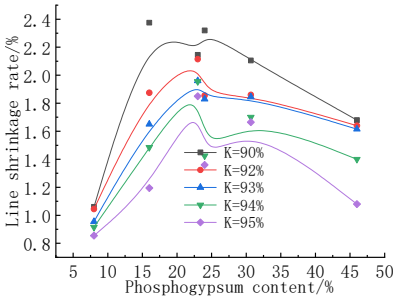


Figure 13. Relationship between linear shrinkage of the mixture and the content of phosphogypsum (L = 8%).

3.5. Microstructure Analysis

To observe the structure of phosphogypsum-stabilized red clay particles and analyze the reasons for the increased strength of the mixture, a Hitachi S-4800 Scanning Electron Microscope at 20,000× magnification was used to scan plain red clay and a phosphogypsum mixture with 8% lime, and analyzed using a Rigaku SmartLab SEX-ray Diffractometer. SEM results are shown in Figure 14. XRD quantitative analyses are shown in Table 8 and Figure 15.

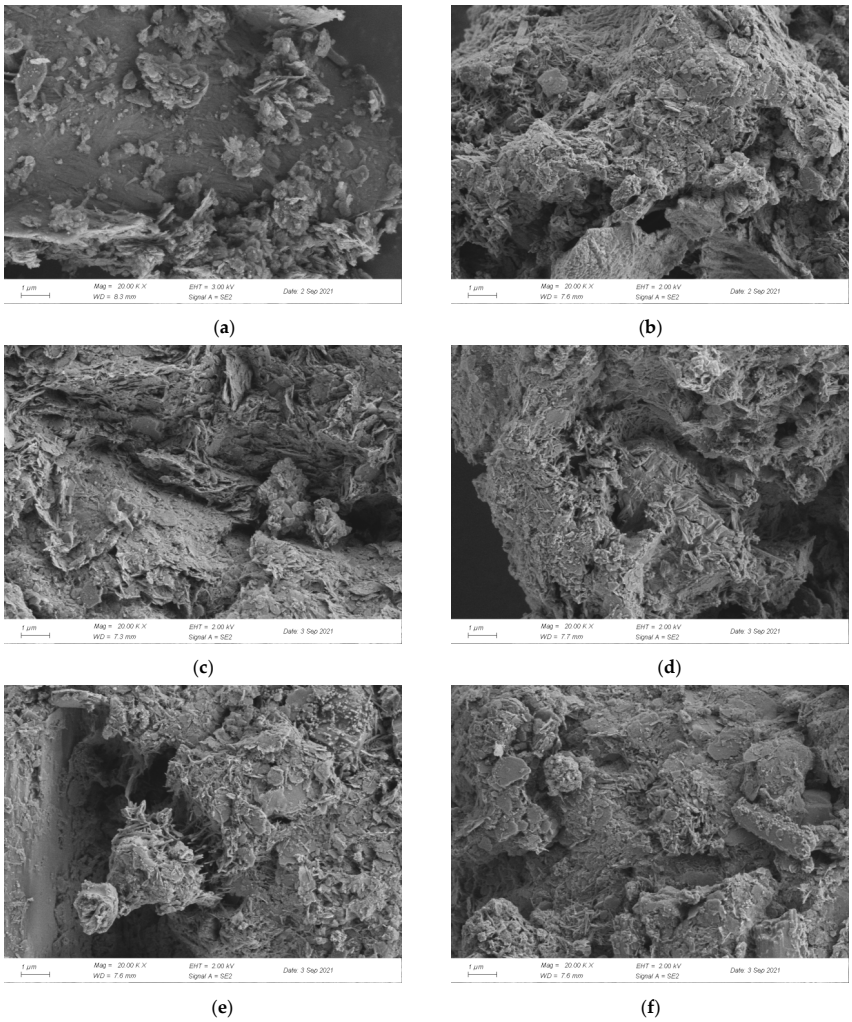


Figure 14. SEM images of plain red clay and stabilized red clay. (**a**) 0%L + 0%P + 100%T; (**b**) 8%L + 8%P + 84%T; (**c**) 8%L + 16%P + 76%T; (**d**) 8%L + 24%P + 68%T; (**e**) 8%L + 31%P + 61%T; (**f**) 8%L + 46%P + 46%T.

Table 8. Quantitative analysis table for compositions of plain red clay and the mixture (L = 8%).

Mineral Phase Content (WT%)	Chemical Formula	Phosphogypsum Content (%)					
		0	**8**	**16**	**24**	**31**	**46**
Quartz	SiO_2	42.8	29.0	21.3	15.6	12.6	10.5
Calcite	$CaCO_3$	0	9.8	7.6	6.9	3.9	5.7
Ettringite	$Ca_6Al_2(SO_4)_3(OH)_{12}\cdot 26H_2O$	0	16.8	13.2	12.4	9.5	6.6
Gypsum	$CaSO_4.2H_2O$	0	9.5	28.5	45.6	61.1	69.6
Kaolinite	$Al_2(OH)_4Si_2O_5$	18.7	0.3	0.2	0.2	0.1	0.1
Goethite	FeOOH	8.8	15.6	13.4	8.0	4.5	2.2
Muscovite	$(K,Na)Al_2(Si,Al)_4O_{10}(OH)_2$	29.7	17.9	15.4	11.4	8.3	5.4
Montmorillonite	$(Na,Ca)_{0\cdot 3}(Al,Mg)_2Si_2O10(OH)_2\cdot nH_2O$	0	1.0	0.5	0	0	0

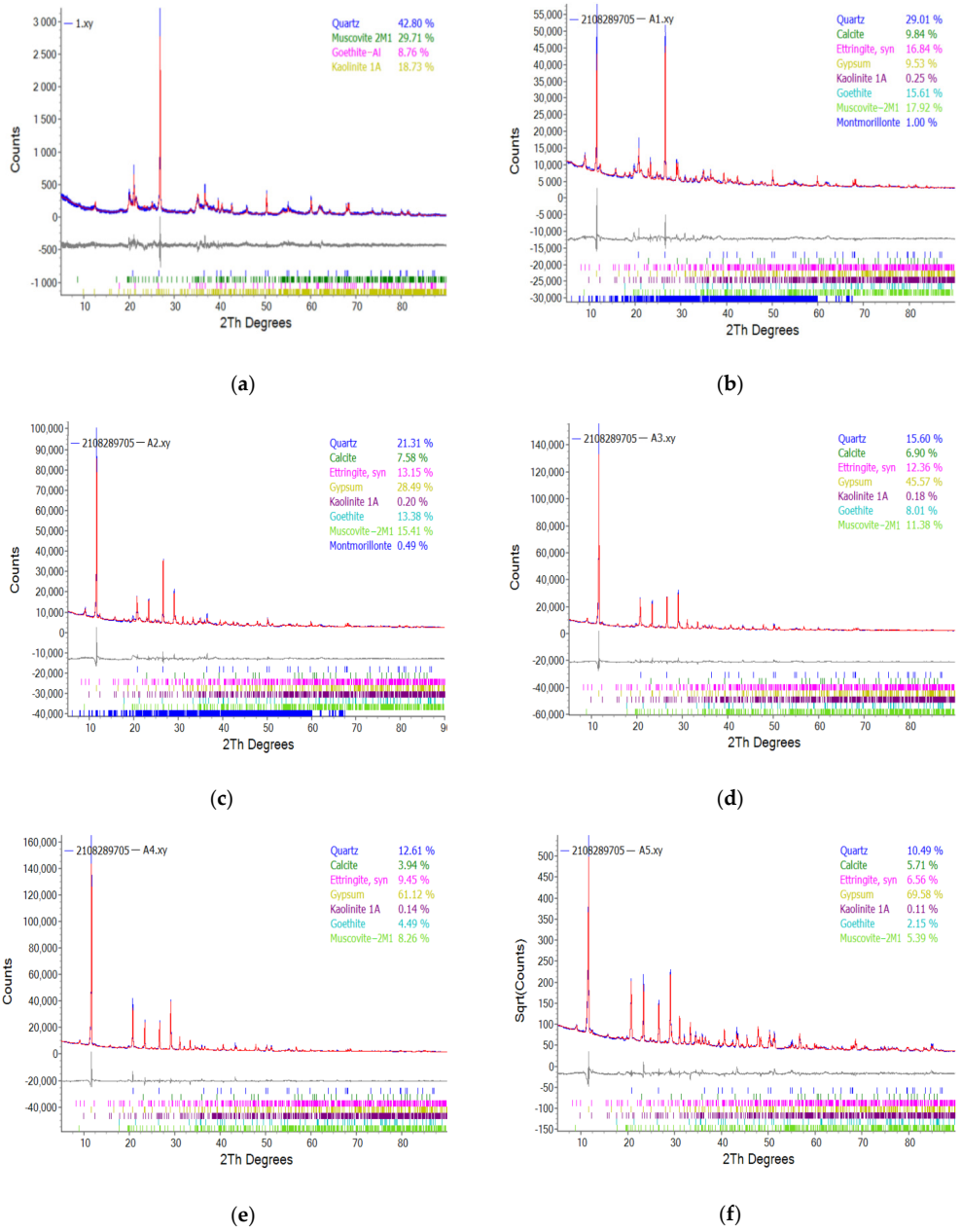


Figure 15. Quantitative analysis of the compound composition of the mixture. (**a**) 0%L + 0%P + 100%T; (**b**) 8%L + 8%P + 84%T; (**c**) 8%L + 16%P + 76%T; (**d**) 8%L + 24%P + 68%T; (**e**) 8%L + 31%P + 61%T; (**f**) 8%L + 46%P + 46%T.

Under certain compaction conditions, a series of physical, physicochemical, and chemical changes occurred in the mixture. The main chemical reaction was alkaline lime reacting with activated silica and activated alumina in the red clay to produce hydrated calcium silicate ($3Ca{\cdot}SiO_2{\cdot}nH_2O$) and hydrated calcium aluminate ($3CaO{\cdot}Al_2O_3{\cdot}nH_2O$). The chemical reactions are as follows:

$$3\ Ca(OH)_2 + SiO_2 + (n - 3)\ H_2O \rightarrow 3\ CaSiO_2{\cdot}nH_2O, \quad (3)$$

$$3\ Ca(OH)_2 + Al_2O_3 + (n - 3)\ H2O \rightarrow 3\ CaAl_2O_3{\cdot}nH2O, \quad (4)$$

This is the reason for the early strength of lime–phosphogypsum-stabilized red clay. The generated hydrated calcium silicate and hydrated calcium aluminate continued to react with phosphogypsum in the mixture to form ($3\ CaO{\cdot}Al_2O_3{\cdot}3CaSO_4{\cdot}32H_2O$), which is what we often call ettringite. The chemical reaction is as follows:

$$3\ CaO{\cdot}Al_2O_3{\cdot}nH_2O + 3\ CaSO_4{\cdot}2H_2O + (26 - n)\ H_2O \rightarrow 3\ CaO{\cdot}Al_2O_3{\cdot}3CaSO_4{\cdot}32H_2O, \quad (5)$$

Figures 14 and 15 and Table 8 show that the shapes of plain soil granules were obvious. With the addition of lime, the reaction produced cemented calcium silicate hydrate and calcium aluminate hydrate, and the soil particles gathered together and provided some strength. Continued addition of phosphogypsum generated ettringite, which filled the pores. In addition, ettringite can be cemented with gelling substances to form a skeleton; the structure is more compact, the pore size is reduced, and the porosity is reduced, which reduces the shrinkage rate of the stabilized soil mixed material and improves its crack resistance. However, excessive ettringite causes breaking of the originally formed skeleton due to excessive expansion, and this results in decreased strength.

When L:P = 1:1, that is, P = 8%, the moisture content of the mixture was 30.24%. Compared with other groups, the moisture content was the largest, and the internal voids were the largest. Based on these results, ettringite is most abundant at this time. After filling a large number of pores, there was still a small amount of excess ettringite that broke the originally formed framework structure, which resulted in a decrease in strength and a small absolute expansion rate. With continuing addition of phosphogypsum, the alkalinity of the environment decreased and the gel performance was poor, and the pH value of the mixture decreased rapidly when the ettringite gradually dissolved. When L:P = 1:3, that is, P = 24%, the moisture content of the mixture was 27.41%, which was relatively low compared to other groups, and the pores between internal particles were not large. These results indicate that excess ettringite was produced at this time. After part of the ettringite swelled to fill the pores, most of the excess ettringite expanded and squeezed the originally formed skeleton structure, resulting in a decrease in strength and expansion. When P:T = 1:2, that is, P = 31%, the water content of the mixture was as small as 27.59%, and the pores between internal particles were not large. From the perspective of strength, the ettringite generated at this time filled the pores well, and there was no excessive expansion that caused breaking of the framework. The expansion was caused by water absorption and expansion of the muscovite, and the strength of the mixture was at a maximum at this time. When P:T = 1:1, that is, P = 46%, the minimum moisture content of the mixture was 25.94%, and the spacing between internal particles was at a minimum. At this time, ettringite abundance was at its lowest level, and there was only a small amount of surplus left after filling the pores. Ettringite caused a small amount of swelling in this case.

From the perspective of water stability, because muscovite, kaolinite, and montmorillonite are hydrophilic, the composition analysis in Table 8 shows that with increases in phosphogypsum, muscovite, kaolinite, and montmorillonite levels, the total amount of stone gradually decreased, the hydrophilicity gradually lessened, and the water stability increased. This also confirms the phenomenon reflected in Figure 8.

4. Discussion

At present, the problems of phosphogypsum resource waste and special engineering characteristics of red clay soil are more prominent. Mixing phosphogypsum with red clay soil by adding lime for road base filler solves the problem of solid waste phosphogypsum piling and improves the bad engineering characteristics of red clay soil, which has important scientific significance and engineering application value. This paper systematically analyzes the road performance of phosphogypsum-stabilized red clay and analyzes its mechanism from the microscopic perspective to provide technical support for the application of phosphogypsum-stabilized red clay in roadbed engineering. However, there are still some problems:

1. Environmental impact of lime–phosphogypsum-stabilized red clay: phosphogypsum contains harmful elements; the main chemical composition is sulfur, phosphorus, and fluorine. According to the phosphogypsum sample test results, sulfur, phosphorus, and fluorine content are in line with the standard, but these elements in the process of mixing with lime and red clay produce physicochemical reactions, the results of the reaction are beyond the standard;, whether the production of leachate is environmentally hazardous is worth devoting sufficient attention to.
2. Lime–phosphogypsum-stabilized red clay water stability and swelling problem: lime–phosphogypsum-stabilized red clay water stability is very poor, basically within 24 h the mixture is completely loose and off, there is basically no strength. Swelling is very great, the expansion rate can reach 55%. Lime–phosphogypsum-stabilized red clay water stability and the swelling problem are the key problems of using it as roadbed filler; it is recommended to consider adding an admixture to solve the water stability and swelling problem.
3. Red clay is widely distributed and spatially variable, and phosphogypsum in different regions also varies, so it is still necessary to conduct a large number of experiments and studies for raw materials in different regions, from which we can draw experience and enrich the aspects of phosphogypsum stabilization of red clay.
4. Under the premise of meeting the requirements of roadbed specifications, compared with lime–fly ash–phosphogypsum mixtures, the strength of lime–phosphogypsum-stabilized red clay is reduced, the amount of phosphogypsum is increased, and the construction cost is greatly reduced. The strength characteristics and deformation characteristics of red clay have been improved. At present, there are few studies on the mechanism of lime–phosphogypsum improving soil performance. This paper analyzes its mechanism from a microscopic point of view and provides theoretical support for the application of lime–phosphogypsum in stabilizing red clay in road engineering.

5. Conclusions

(1) The unconfined compressive strength of the mixture first increased and then decreased with increasing phosphogypsum content. The higher the lime content was, the greater the unconfined compressive strength of the mixture. With increasing age, the unconfined compressive strength of the mixture increased faster in the first 14 days and slower in the latter 14 days. The water stability of the mixture was poor.

(2) When the lime content was 8%, the absolute expansion rate of the mixture increased with time, and the expansion had not yet reached stability at 223 h. At this time, the absolute expansion rates of the mixtures with different phosphogypsum contents ranged from 38% to 55%. The greater the degree of compaction was, the greater the absolute expansion rate of the mixture. The absolute expansion rate of the mixture first increased and then decreased with increasing phosphogypsum content.

(3) The linear shrinkage rate of the mixture increased rapidly with time, then increased slowly and finally stabilized. With increasing phosphogypsum content, it first increased and then decreased. The line shrinkage rate was between 0.8 and 2.2%.

(4) With the addition of lime, the hydration reaction produced calcium silicate hydrate and calcium aluminate hydrate, which gathered the soil particles together and increased the strength. Continuous addition of phosphogypsum generated ettringite, which exhibited swelling and filled pores and was cemented with gelling substances to form a skeletonS that further increased the strength. However, excessive ettringite caused the originally formed skeleton to be broken due to excessive expansion, resulting in a decrease in strength. Second, with increases in the phosphogypsum content, the total amount of muscovite, kaolinite, and montmorillonite gradually decreased, the hydrophilicity gradually weakened, and the water stability improved.

Author Contributions: Conceptualization, K.-S.C.; Methodology, K.-S.C.; Software, Z.-Y.L.; Formal analysis, Z.-Y.L.; Data curation, Z.-Y.L.; Writing—original draft, Z.-Y.L.; Writing—review and editing, K.-S.C.; Supervision, K.-S.C.; Project administration, K.-S.C. All authors have read and agreed to the published version of the manuscript.

Funding: This research was funded by Guizhou Provincial Science and Technology Project (Qianke He basical -ZK[2023] No. key 016; Qianke He Support [2020] No. 4Y038).

Institutional Review Board Statement: Not applicable.

Informed Consent Statement: Not applicable.

Data Availability Statement: The data used to support the findings of this study are included in the article.

Conflicts of Interest: The authors declare no conflict of interest.

References

1. Zhang, H.Q.; Xu, X.; Hu, C.J.; Zhou, F. Current situation of comprehensive utilization technology of solid waste of phosphorous chemical. *China Min. Mag.* **2021**, *30*, 50–55+63.
2. Zhu, Z.; He, D.S.; Chen, F.; Zhang, K.C.; Wang, Q.Y. Research progress on pretreatment and comprehensive utilization of phosphogypsum. *Conserv. Util. Miner. Resour.* **2019**, *39*, 19–25.
3. Shang, K. Research progress on pollution in situ control and ecological restoration of phosphogypsum yard. *Guangzhou Chem. Ind.* **2015**, *43*, 42–43.
4. Tong, J. Present situation and prospect of phosphogypsum treatment and disposal during the 13th five-year Plan. *Dev. Orientat. Build. Mater.* **2018**, *16*, 6–11.
5. Wang, J.S.; Li, Y.M.; Wang, G.X.; Zhao, X.P. Experimental study on engineering characteristics of red clay in southwest mountainous area. *Subgrade Eng.* **2013**, *6*, 97–101.
6. Wang, Y.F.; Hu, H.H.; Ma, D.Q. Engineering characteristics of residual red clay in Hunan and its influence on highway construction. *Hunan Commun. Sci. Technol.* **2016**, *42*, 14–17.
7. Wang, Z.W.; Hong, B.N.; Liu, X. Water-sensitivity properties of shear strength of red clay. *J. Sichuan Univ. Adv. Eng. Sci. J.* **2011**, *43*, 17–22.
8. Jiang, H.; Jiang, H.; Chen, K.S.; Ji, Y.X. Investigation on Slope Diseases of Red Clay Highway in Jiangxi Province. *J. Guizhou Univ. Nat. Sci. Ed.* **2019**, *36*, 109–113.
9. Pu, S.W. Study on the influence of water content on the shear strength of red clay in different states. *J. Guizhou Univ. Nat. Sci. Ed.* **2019**, *36*, 93–100.
10. Thakur, Y.; Tyagi, A.; Sarkar, S. Utilization of Industrial Waste Phosphogypsum as Geomaterial: A Review. *J. Hazard. Toxic Radioact. Waste* **2023**, *27*, 1181. [CrossRef]
11. Liu, Y.T.; Zhang, D.R.; You, L.Y.; Luo, H.; Xu, W. Recycling phosphogypsum in subbase of pavement: Treatment, testing, and application. *Constr. Build. Mater.* **2022**, *342*, 1–14. [CrossRef]
12. Arunvivek, G.K.; Rameshkumar, D. Experimental Investigation on Feasibility of utilizing Phosphogypsum in E-Glass Fiber-incorporated Non-fired Ceramic Wall Tile. *J. Inst. Eng. India Ser. A* **2022**, *103*, 445–451. [CrossRef]
13. Diouri, C.; Echehbani, I.; Lahlou, K.; Omari, K.; Alaoui, A. Valorization of Moroccan phosphogypsum in road engineering: Parametric study. *Mater. Today Proc.* **2022**, *58*, 5. [CrossRef]
14. Manjit, S. Treating waste phosphogypsum for cement and plaster manufacture. *Cem. Concr. Res.* **2002**, *32*, 1033–1038.
15. Degirmenci, N. Utilization of phosphogypsum as raw and calcined material in manufacturing of building product. *Constr. Build. Mater.* **2008**, *22*, 1857–1862. [CrossRef]
16. Li, S.; Wang, D.; Tang, C.; Chen, Y. Optimization of synergy between cement, slag, and phosphogypsum for marine soft clay solidification. *Constr. Build. Mater* **2023**, *374*, 13. [CrossRef]

17. Wang, H.J.; Shi, M.L.; Tian, X.T.; Yu, C.Y.; Du, X.Y. Experimental Study on Phosphogypsum-Amended Red Mud as Road Base Material. *Sustainability* **2023**, *15*, 1719. [CrossRef]
18. Meskini, S.; Remmal, T.; Ejjaouani, H.; Samdi, A. Formulation and optimization of a phosphogypsum-fly ash-lime composite for road construction: A statistical mixture design approach. *Constr. Build. Mater* **2022**, *315*, 11. [CrossRef]
19. Dutta, R.K.; Khatrib, V.N.; Panwara, V. Strength characteristics of fly ash stabilized withlime and modified with phosphogypsum. *J. Build. Eng.* **2017**, *14*, 32–40. [CrossRef]
20. Kumar, S.; Dutta, R.K.; Mohanty, B. Engineering Properties of Bentonite Stabilized withLime and Phosphogypsum. *Slovak J. Civ. Eng.* **2015**, *22*, 35–44. [CrossRef]
21. Kargar, S.; Javadi, A.A.; Estabragh, A.R. Investigation on the mechanical properties of gypsum soil. *Constr. Mater.* **2014**, *167*, 251–257.
22. Tang, Q.Q.; Ling, T.Q.; Dong, M.S. Application of industrial waste phosphogypsum in roadbed and pavement engineering. *J. Shandong Jiaotong Univ.* **2002**, *2*, 49–52.
23. Xu, X.Y. A Sutdy On Engineering Chaarcteristics of Phosphoygpsum And its Mixuters. Master's Thesis, Hohai University, Nanjing, China, 2005.
24. Xu, X.Y.; Xu, Y.Z.; Chen, G.S.; Yu, X.J.; Zhu, J.H. Testing study on the shrinkage property of phosphogypsum-fly ash-lime-clay. *Highw. Eng.* **2006**, *4*, 113–114+119.
25. Xu, X.Y.; Xu, Y.Z.; Chen, G.S.; Yu, X.J. Testing study on engineering characteristics of phosphogypsum. *Chin. J. Rock Mech. Eng.* **2004**, *12*, 2096–2099.
26. Ministry of Transport of the People's Republic of China. *Technical Guidelines for Construction of Highway Roadbases*; JTG/T F20-2015, People's Communications Press: Beijing, China, 2015.
27. Hu, W.H.; Liu, C.Q.; Liu, Z.Q.; Liu, D. Experimental study on mechanical strength properties of cement or lime modified red clay. *Subgrade Eng.* **2017**, *5*, 11–14+19.
28. Zhang, Y.F.; Tong, H.M.; Shen, W.G.; Pan, H.X.; Shi, Y. Research on waste gypsum-fly ash-lime binder. *World Build. Mater.* **2009**, *30*, 45–47+59.
29. Yang, H.P.; Li, H.Q. Experimental study on the road properties of high liquid limit soil improved by lime. *Highw. Eng.* **2013**, *38*, 227–229.
30. Wa, H. Research of the Application of Pavement Base Material with Phosphorus Slag (Phosphogypsum). Master's Thesis, Chongqing Jiaotong University, Chongqing, China, 2008.
31. Song, T. Study on the Performance of Road Packing with Industrial Residues of Phosphogypsum. Master's Thesis, Wuhan Polytechnic University, Wuhan, China, 2012.
32. *ASTM D2166/D2166M*; Standard Test Method for Unconfined Compressive Strength of Cohesive Soil. American Society for Testing and Materials: Filadelfia, PA, USA, 2016.
33. Ministry of Transport of the People's Republic of China. *Test Methods of Soils for Highway Engineering*; JTG 3430-2020; People's Communications Press: Beijing, China, 2020.

Disclaimer/Publisher's Note: The statements, opinions and data contained in all publications are solely those of the individual author(s) and contributor(s) and not of MDPI and/or the editor(s). MDPI and/or the editor(s) disclaim responsibility for any injury to people or property resulting from any ideas, methods, instructions or products referred to in the content.